The Design and Performance of an Electronic Torque Standard Directly Traceable to the Revised SI

Zane Comden, John Draganov, Stephan Schlamminger, *Senior Member, IEEE*, Frank Seifert, Charles Waduwarage Perera, David B. Newell, and Leon S. Chao

***Abstract*— The United States National Institute of Standards and Technology (NIST) has been developing a new device for primary standard realization of torque utilizing established traceability to quantum-electrical standards following the 2019 revision of the International system of units (SIs). This device, the Electronic NIST Torque Realizer (ENTR) is a device directly traceable to the quantum-electrical standards of the revised SI with the goal of outperforming current commercial torque transducer uncertainty levels, improving torque tool calibration at low torque ranges, and shortening the torque standards dissemination chain. This project's goal is to create a device for torque calibrations with an operational range of 7×10^{-4} N m to 1 N m with uncertainty at or below 0.1%. We intend ENTR to be a possible replacement for present transfer standards used in the torque standards dissemination chain, easing the financial and logistical burdens of current torque standards dissemination systems.**

***Index Terms*— Calibration, measurement techniques, measurement uncertainty, metrology, torque measurement.**

I. Introduction

AFTER the 2019 revision of the International System of Units (SIs), the kilogram is now defined by the exact value of Planck's constant and can be realized via quantum-electrical standards, one method utilizing the Kibble principle [1].

Now, torque no longer needs to be traceable to a calibrated weight suspended from a known lever arm. Specifically, a modification of the Kibble principle used for realizing the kilogram allows for the direct realization of torque via electrical measurements traceable to the revised SI [2], [3], [4]. Progress on table-top sized Kibble balances at national metrology institutes such as the National Institute of Standards and Technology (NIST) of the U.S. [5] and Physikalisch-Technische Bundesanstalt of Germany [6], has inspired a similar device capable of realizing torque with SI traceability to quantum-electrical standards.

For torque lower than 1×10^{-2} N m, balancing small mass artifacts required to calibrate fragile transducers is difficult, burdensome, and often irreproducible. A collaborative effort between NIST and the U.S. Air Force to design, construct, and characterize a Kibble-style electromechanical system for directly calibrating torque tools is currently under development.

This effort's goal is to create a tabletop-sized electromagnetic torque calibration device capable of generating 7×10^{-4} N m to 1 N m with 0.1% uncertainty.

We note that this value of accuracy is significantly larger than uncertainty levels achieved by previous work from other national metrology institutes [2], [3]. This device, the Electronic NIST Torque Realizer (ENTR) is designed for robustness, commercial utilization, simplicity, and affordability. A primary goal of the project is to insert a quantum-electrical standard traceable device as far downstream in the traceability chain as possible, removing the necessity for calibrated masses and length standards in torque calibrations. ENTR is intended to re-route the SI standards dissemination chain from mechanical to quantum-electrical standards, empowering calibration facilities ranging from military to research and industry to directly realize torque for themselves.

This publication is an extended version of a proceedings article from the 2022 Conference on Precision Electromagnetic Measurements [7]. In the following text, we describe the theory, the apparatus, and show the first result.

II. Theory

Forces and torques are related phenomena. Forces change linear momentum while torques change rotational momentum. Hence, it is not surprising that applying the Kibble principle to a rotational system can be used to realize torque just as a linear Kibble balance realizes force. In previously designed Kibble balances such as the NIST-4 Kibble balance, a coil is translated vertically through a fixed magnet system [8]. For the rotational version, a magnet system spins with respect to a fixed coil. Theoretically, the system could be constructed from a rotating coil with a stationary magnet system, but this was not chosen for this project due to foreseen complications with wiring and electrical connections.

Still, the measurement requires two modes of operation: spin mode

$$V = BLr\omega \tag{1}$$

Manuscript received 1 February 2023; revised 7 April 2023; accepted 1 May 2023. Date of publication 25 May 2023; date of current version 14 June 2023. This work was supported by the National Institute of Standards and Technology and the U.S. Air Force. The work of John Draganov was supported by the Professional Research Experience Program (PREP) between the National Institute of Standards and Technology (NIST) and the University of Maryland, College Park under Agreement 5275372. The Associate Editor coordinating the review process was Dr. Shisong Li. *(Corresponding author: Zane Comden.)*

Zane Comden, Stephan Schlamminger, David B. Newell, and Leon S. Chao are with the National Institute of Standards and Technology, Gaithersburg, MD 20899 USA (e-mail: zcomden@gmail.com).

John Draganov was with the Department of Chemistry and Biochemistry, University of Maryland, College Park, MD 20742 USA. He is now with the National Institute of Standards and Technology, Gaithersburg, MD 20899 USA.

Frank Seifert is with the National Institute of Standards and Technology, Gaithersburg, MD 20899 USA, and also with Joint Quantum Institute, University of Maryland, College Park, MD 20742 USA.

Charles Waduwarage Perera was with the National Institute of Standards and Technology, Gaithersburg, MD 20899 USA, and also with the Department of Chemistry and Biochemistry, University of Maryland, College Park, MD 20742 USA. He is now with the Goddard Space Flight Center, Greenbelt, Maryland.

Digital Object Identifier 10.1109/TIM.2023.3279911

and torque mode

$$\tau_a = BLrI \tag{2}$$

where V is the induced voltage in the coil from the spinning magnet, B is the magnetic flux density of the magnetic circuit, L is the total length of the radial wire segments of the coil, and r is the distance between the axis of rotation and the center of each wire segment. We define ϕ as the angular position of the magnet system, and $\omega = \dot{\phi}$ as the angular velocity. The torque τ_a is applied externally from a device that is to be calibrated and the servo system adjusts the current I in the coil to maintain it at a fixed angle ϕ_o. The magnetic coupling factor, BLr, which we abbreviate in the following with β is a function of angular position ϕ, i.e., the relative position between coil and magnet. The induced voltage is not only a function of ϕ, but also time since the velocity of the rotating magnet is slowly decreasing due to friction

$$V(t, \phi) = \beta(\phi)\omega(t, \phi). \tag{3}$$

From a fitting procedure, outlined below, to the quotient of pairs of measurements $V(t, \phi)/\omega(t, \phi)$, taken at the same time and angle, the value of $\beta(\phi_o)$ at the angle ϕ_o can be obtained. In the division of the voltage by the angular velocity, the time dependence cancels and β only depends on the angle. Hence, the measured torque is given by

$$\tau_m = I\beta(\phi_o) = \frac{IV(\phi_o)}{\omega(\phi_o)}. \tag{4}$$

The remainder of this article explains the mentioned steps in detail and discusses the measured agreement between τ_a and τ_m.

III. Design and Construction

A. Mechanical Design

The ENTR mechanical components consist of a central rotor, two ceramic ball bearings, a base plate, and an upper cantilever structure. One bearing sits in the base plate, while the other rests in the cantilever structure, and both constrain the motion of the central rotor. The base plate and cantilever are fabricated from an acetal plastic to maintain structural rigidity without influencing the magnetic field generated by the NdFeB magnets of the central rotor. A rendering of ENTR is shown in Fig. 1.

For the NdFeB magnets, two ring-shaped magnets were cut along a diameter. One-half of each magnet was flipped upside down, and the magnets were placed on the steel yokes and affixed to the central rotor, oriented in attraction. A detailed rendering of the rotor is visible in Fig. 2. We chose to rotate the magnet instead of the coil to avoid electrical connections to the rotor, which may have produced unwanted torques and friction.

Radial alignment of the bearings is ensured by tight machining tolerances between the cantilever with the base plate. Both parts have an arc cut out of equal radius concentric to the bearing locations. Ceramic ball bearings were chosen as they had the lowest friction out of a sample of bearings tested, including stainless steel, hybrid, and angular contact ceramic bearings. Air bearings were determined not to be appropriate for this initial prototype due to practical reasons such as requiring an active air hose and higher cost.

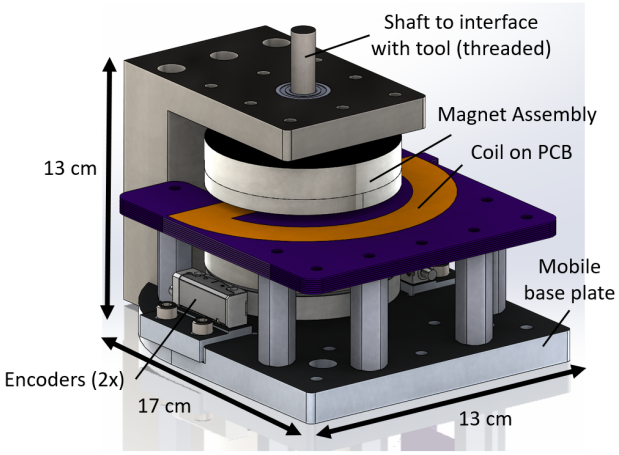

Fig. 1. Assembly drawing of the ENTR.

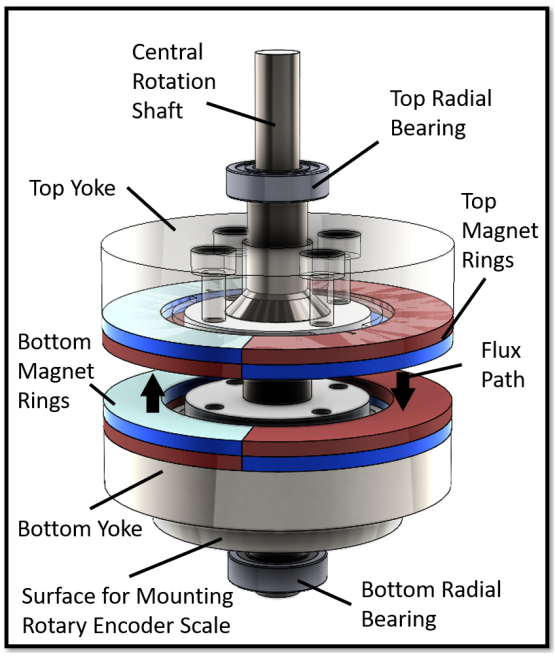

Fig. 2. Detail image of ENTR's central rotor. Magnet poles are colored to indicate the flux path direction.

B. Electromagnetic Design

For ease of construction, the electromagnetic coil is constructed from a stack of identical printed circuit boards (PCBs).

A drawing of the top side of one PCB is shown in Fig. 3. Current flows from the conductive pad at the top of one board along the traces in the top layer, then through a via to the bottom layer of the PCB. The current then follows a path in the same direction along the trace on the bottom side of the board until it reaches a conductive pad at the same location as the top conductive pad on the opposite side of the board. Because of the identical pad locations, these PCBs can be stacked and soldered with the current moving from one PCB to the next. Eight boards are connected by soldering at the pad locations and securing the assembly with polyimide tape. The stack of PCBs is then placed in an oven to re-melt the solder and ensure the electrical connections.

Fig. 3. 3-D model of one PCB that comprises the electromagnetic coil. Each PCB contains two layers with 33 turns on each layer. Each board has an identical connection pad on the opposite side at the location of the red circle (top), and a via connects the two sides of the board at the location of the blue circle (left). Multiple boards are connected by stacking them and placing solder between the connection pads of each board.

C. Data Acquisition

The primary data acquisition device (DAQ) is a National Instruments universal serial bus (USB)-6351 Multifunction I/O Device[1] (Hereafter referred to as "the DAQ"). Voltage measurements are made with a Keysight 34465A digital voltmeter (DVM), and angular position measurements are made with a dual-readhead Renishaw VIONiC encoder system. The encoder scale has a 20 μm graduation and the encoders utilize 500$\times$ interpolation to give a resolution of 40 nm. The encoder output signal is 20 MHz. Two readheads are used to minimize systematic effects caused by the runout of the encoder disk. The signals of both encoders are combined at hardware using a component provided by the manufacturer to a quadrature signal that is digitized by the DAQ. Voltage and position measurements are synchronized by a 400 Hz clock generated by the DAQ. Position data from the optical encoder is received through the DAQ, while voltage data is recorded in the internal buffer of the DVM and read via USB.

IV. Measurement Procedure and Operation

A. Spin Mode

In spin mode, the value of β is determined by driving the rotor to a target angular velocity, $\omega_{\max} = 6.1$ rad s by driving a current through the electromagnetic coil, where the current is modulated with a simple angular position feedback loop. After reaching $\omega_{\max}$, the rotor is allowed to freely spin while measurements of voltage and angular position are taken. After reaching a set minimum angular velocity, $\omega_{\min} = 3$ rad s^{-1}, data collection is paused. These values of $\omega_{\max}$ and $\omega_{\min}$ are chosen as to ensure the speed limit of the angular encoder is not exceeded, and an adequate number of data points are taken per revolution. The voltage and position data taken within $\omega_{\max}$ to $\omega_{\min}$ are recorded for a profile fit as discussed below. The rotor is then driven in the opposite direction to $-\omega_{\max}$ and data is collected until $-\omega_{\min}$.

[1]Certain commercial equipment, instruments, and materials are identified in this article in order to specify the experimental procedure adequately. Such identification is not intended to imply recommendation or endorsement by the NIST, nor is it intended to imply that the materials or equipment identified are necessarily the best available for the purpose.

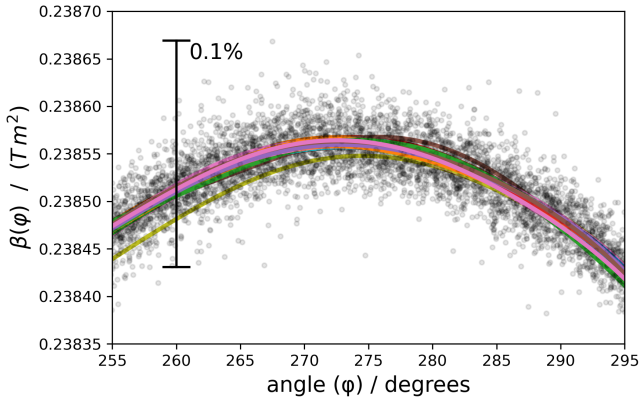

Fig. 4. Spin mode fitting over 76 rotations with 76 fits applied. The scale bar on the left of the plot shows a range of 0.1% of the average value of the fits at $\phi = 275°$.

The process is automatically repeated giving as many values of β as desired until stopped by the operator. When the operator chooses to end the calibration, ENTR stops taking data and a Python script calculates the value of β for a chosen angle ϕ_o. From experience, a typical spin mode session includes about 240 magnet revolutions in both clockwise and counterclockwise directions spanning about 15 minutes. Each individual rotation's β profile is fit with a 6° polynomial (Fig. 4) in the region of interest about ϕ_o. These values are then averaged to give one $\beta(\phi_o)$ value per "spin-down" from $\pm\omega_{\max}$ to $\pm\omega_{\min}$. ENTR then switches into torque mode.

B. Torque Mode

Upon entering torque mode, the electrical circuit of the system is changed such that the voltmeter measures the current through the electromagnetic coil via the voltage drop across a known resistor connected in series with the electromagnetic coil and the current source.

Closed-loop angular position control is used to rotate the magnet assembly to the angle ϕ_o at which β has been calculated. As the rotor of the magnet assembly is held at the desired position by the control loop, any torque applied to the rotor is counteracted by a torque generated by the current through the coil.

The electromagnetic torque produced by the current can be calculated using (4), where $\beta(\phi_o)$ is determined from the average of the preceding and following spin mode values.

C. Comparison to Present Standard

A key design feature of ENTR is its ability to operate horizontally. This allows for a direct comparison between the electromagnetically produced torque of ENTR and the torque produced by known masses on known lever arms. Utilizing this feature, we perform an experiment comparing ENTR to a "dead-weight" torque standard; presently the standard process for calibrating torque transducers at the national metrology institute level.

A truncated wheel of $2r_w = 508$ mm diameter is mounted to the shaft of ENTR, while care is taken to align the shaft horizontally in the lab.

A 50 g mass hanger is suspended from a fiber with a diameter ($2r_f = 0.30$ mm) off each end of the truncated wheel. Three wire masses m_x, ($x \in \{1, 2, 3\}$) can be placed on either hanger to produce a known torque, τ_a, applied to

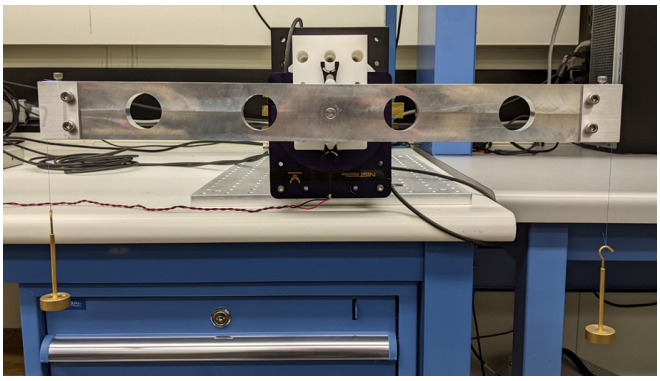

Fig. 5. Photograph of the torque verification mode with length standard affixed to ENTR in the horizontal orientation.

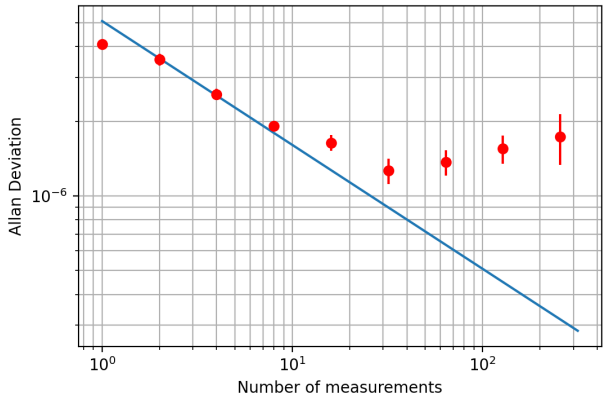

Fig. 6. Relative Allan Deviation plot of 913 consecutive A-B-A sets of torque measurements taken over approximately 40 h. The horizontal axis is expressed in a number of measurements to display how many measurements are required to achieve a statistically significant measurement of torque.

ENTR's rotary shaft. By placing the wire mass on the hanger the change in torque is

$$\tau_a = m_x g(r_f + r_w). \tag{5}$$

Here g is the local gravitational acceleration in the laboratory. The value of $g = 9.80101$ m/s^2 was taken from an NOAA website with a relative uncertainty of 2×10^{-6}.

The value of torque generated by the mass on the lever arm is compared to the torque reported by ENTR, τ_m. A photograph of the torque verification assembly is shown in Fig. 5.

Measurements are conducted in an A-B-A-B-A... style of data collection. Measurements of torque on the rotor having no mass (A) on the hanger are alternated with measurements of torque with the wire mass on the hanger (B). A total of 31 measurements per mass per side are taken, each lasting 20 s and containing approximately 2200 voltage data points. We choose these measurement parameters to achieve a statistically significant torque value for each A or B measurement. Placement and removal of the wire test masses are automated using a linear stage and stepper motor system, removing irreproducible human effects in placing and removing the masses.

A friction hysteresis erasing procedure is also performed before each measurement. We borrow a technique for hysteresis erasing used in Kibble balances for decades. Robinson [9] in 2012 describes a hysteresis erasing procedure for a Kibble balance utilizing a knife edge, and we adapt the technique for a ball-bearing-constrained rotor. After an excursion occurs in a mechanical pivot due to a load change, the pivot is exercised consistently regardless of the load change. In this case, the rotor is driven in a decaying sinusoidal fashion with an initial amplitude of 2°, while typical excursions of the rotor during mass placement and removal are approximately 0.1°. This erasing procedure reduces a possible systematic error due to inelastic forces and torque on the pivot.

Three masses are used in the comparison experiment with nominal values of $m_1 = 500$ mg, $m_2 = 3$ g, and $m_3 = 8$ g. The mass values are determined with a series of measurements on mass comparators. These masses are chosen to cover the lower range of the operational goals as we foresee the greatest difficulty in achieving the desired uncertainty at the lowest operational ranges of ENTR.

V. Uncertainty Analysis

A. Repeatability of Measurement

To determine uncertainty due to the repeatability of torque measurements, an experiment is conducted in which a wire mass is repeatedly placed on and removed from one hanger to measure applied torques and null measurements. 913 pairs of applied torque and null measurements are taken over the course of approximately 40 h. The Allan deviation of the repeatability measurement study is shown in Fig. 6. From this Allan deviation plot, we believe 80 measurements in the present verification experiment set up to be acceptable in order to achieve reasonable levels of type A uncertainty.

B. Encoder Uncertainty

Uncertainty in the angular encoder measurement creates uncertainty in the value of $\beta(\phi)$ determined in spin mode and is found to contribute approximately 1×10^{-7} N m of uncertainty in the measured torque. This uncertainty value is obtained by the value given in the manufacturer's specifications for installed encoder accuracy with proper alignment of the encoder confirmed by an alignment device provided by the manufacturer.

C. Voltage Measurement and Resistance

Voltage measurement uncertainty for the spin mode and the torque mode contribute a combined uncertainty of 3×10^{-7} N m. These values of voltage measurement uncertainty are calculated with consideration of the measurement range and integration time settings of the voltmeter using values provided by the manufacturer. The value of the resistor used in the torque measurement is well-known and contributes only 1×10^{-8} N m of uncertainty.

D. Data Acquisition Hardware Timing

In order to characterize the veracity of the measurement timing system, a virtual quadrature encoder signal is generated using a waveform generator and fed into the DAQ to mimic an encoder with constant velocity. The theoretical velocity of the reference signal is compared to the velocity values calculated by position data taken from the DAQ. The discrepancy between these values gives an uncertainty due to measurement timing of approximately 91 parts in 10^6. This corresponds to a torque measurement uncertainty of 1×10^{-7} N m. A second systematic associated with timing occurs when the voltage and velocity measurements are not perfectly aligned in time. The geometric factor is obtained correctly

using $\beta = V(t_V)/\omega(t_\omega)$ when the two measurement times are identical, $t_V = t_\omega$. In reality, however, there is sampling jitter on the voltage measurement, $t_V = t_\omega + \delta t$, where δt is a random number from a normal distribution with mean zero and standard deviation σ_δ. We estimate that effect to contribute a relative uncertainty of 5×10^{-6}.

E. Data Analysis and Curve Fitting

During the data analysis process, each individual rotation has a calculated β value determined at the chosen angle ϕ_o by fitting a sixth-order polynomial within the region of interest to the values of $\beta(\phi)$. Various fitting algorithms were tested with no significant difference in the calculated $\beta(\phi_o)$ value. The fitting process was determined to contribute approximately 1×10^{-7} N m of uncertainty to the torque measurement.

F. Applied Torque Uncertainty for Verification

Uncertainty in the value of torque applied to the rotor during the verification must also be included in the uncertainty analysis.

The length standard used for verification is measured on a coordinate-measuring machine to a nominal diameter of 508 mm with an uncertainty of 3 μm.

While the diameter of the length standard wheel ($2r_w$) is well known, there is uncertainty in the actual lever arm applying the torque, δr_w, as the true location of the center mounting hole of the length standard is not known exactly. The noncentered hole creates an effect where the torque applied on one side of the length standard wheel is higher than expected from an expected 254 mm lever arm, and the other side will have a lower torque than expected. Thus (5) becomes

$$\tau_a = m_x g\left(r_f + r_w \pm \delta r_w\right) \tag{6}$$

where $\pm$ evaluates to $+$ for clockwise and $-$ for counterclockwise torques.

By taking the difference in the values of torque measured on each side of the bar for the same applied mass, we approximate an additional uncertainty in the lever of 1.9×10^{-5} m due to the δr_w factor.

Furthermore, the uncertainty in the measurement of the radius of the fiber suspending the mass hangers contributes an additional 3×10^{-8} N m of uncertainty in torque applied. Mass measurement remains the greatest source of type B uncertainty in the comparison measurement.

The total absolute uncertainty in torque applied for the lowest value under test is 480×10^{-9} N m of torque. Table I presents the total relative uncertainties for the lowest torque value tested in the verification experiment.

VI. Results and Discussion

Results of the comparison experiment are shown in Fig. 7 and Table II. We perform a first-degree least squares fit taking into account uncertainties in both the measured torques and the applied torques, see [10]. The fit line with uncertainties applied gives an overall agreement between measured and applied torques of 0.051%.

While the lowest torque applied in this comparison (1.18×10^{-3} N m) does not reach the minimum of the operational range goal (7×10^{-4} N m), it offers significant insight into the largest contributing factors of uncertainty in the measurement, namely the repeatability of the measurement and the uncertainty in the voltage measurement. In the future development of ENTR, focus will be placed on reducing these uncertainties to reach the desired goal of 0.1% relative uncertainty for a coverage factor of $k = 2$.

TABLE I

Table of Relative Uncertainties for a 1.18×10^{-3} N m Torque Verification Measurement. All Numbers Are 1σ Uncertainties. Entries Indicated by <0.01 Have Relative Uncertainties That Are Below 10^{-5}

Source	Symbol	rel. unc. $\frac{\tau_a}{1 \times 10^{-3}}$	rel. unc. $\frac{\tau_m}{1 \times 10^{-3}}$
Repeatability	V/R		0.52
Voltage measurement	V		0.24
Profile fitting	$\beta(\phi_o)$		0.12
Encoder	ϕ		0.12
Hardware timing	Δt		0.09
Resistor	R		0.01
DVM sample jitter	δt		<0.01
Mass measurement	m_x	0.40	
Mount hole location	δr_w	0.07	
Diameter of wheel	$2r_w$	0.07	
Radius of fiber	r_f	0.03	
Local acceleration	g	<0.01	
Totals	τ	**0.41**	**0.60**

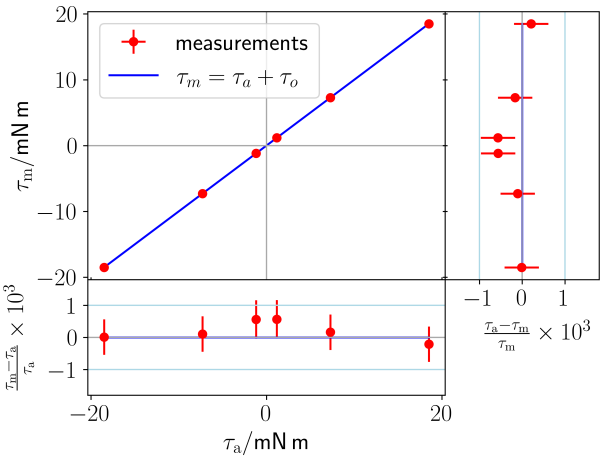

Fig. 7. Results of the comparison experiment. τ_a is torque applied to the rotor by the hanging masses on the lever arm, τ_m is torque measured by ENTR. The solid line represents $\tau_m = \tau_a$. The right-most plot show residuals of the torque applied values against the $\tau_m = \tau_a$ line, while the bottom-most plot shows the residuals of torque measured values against the $\tau_m = \tau_a$ line. Uncertainty bars correspond to the 1σ uncertainties for each measurement.

TABLE II

Results for the Verification Experiment Corresponding to Fig. 7. The First Two Columns Show the Applied, τ_a, and Measured, τ_m, Torques. A Positive Sign Indicates a Clockwise Torque. The Third Column Gives the Difference. The Uncertainties Are for One Standard Deviation, $k = 1$

Torque applied $\frac{\tau_a}{1 \times 10^{-3}\ \text{N m}}$	Torque measured $\frac{\tau_m}{1 \times 10^{-3}\ \text{N m}}$	difference $\frac{\tau_a - \tau_m}{1 \times 10^{-6}\ \text{N m}}$
-18.505 ± 0.008	-18.505 ± 0.010	0 ± 13
-7.292 ± 0.003	-7.293 ± 0.004	1 ± 5
-1.1776 ± 0.0005	-1.1783 ± 0.0007	0.7 ± 0.9
1.1776 ± 0.0005	1.1781 ± 0.0007	-0.6 ± 0.9
7.292 ± 0.003	7.293 ± 0.004	-1 ± 5
18.505 ± 0.008	18.501 ± 0.010	4 ± 13

VII. Conclusion

The goal of this project is to build a device that can calibrate torques of order 1 mN m with relative uncertainties below 1×10^{-3}. Fig. 7 clearly indicates this goal has been met for the torque values tested as the mean value of all measurements falls within the required range, and total measurement uncertainty is well below 0.1%. While the uncertainty values for τ_m are higher than that of τ_a (see Table II), the τ_m values have significantly less uncertainty than presently used torque transfer standards such as commercial torque transducers, indicating ENTR demonstrates significantly greater performance while offering a shorter path in standards dissemination.

In addition, as a computer-controlled device, ENTR is easy to use and keeps a digital data log of the calibrated torque values. Further developments of the project will result in an expanded operational range, as it is easier to reach the uncertainty and accuracy goals for torques larger than 1.8×10^{-2} N m, the largest torque value tested in this experiment.

Acknowledgment

The authors would like to thank Dr. Vincent Lee of the NIST Dimensional Metrology Group, the members of the NIST Mass and Force Group, Alireza Panna of the Fundamental Electrical Measurements Group, and Dr. Stephan Cular of the Applied Electrical Metrology Group for their assistance.

References

[1] I. A. Robinson and S. Schlamminger, "The Watt or Kibble balance: A technique for implementing the new Si definition of the unit of mass," *Metrologia*, vol. 53, no. 5, pp. A46–A74, Sep. 2016.

[2] A. Nishino, K. Ueda, and K. Fujii, "Design of a new torque standard machine based on a torque generation method using electromagnetic force," *Meas. Sci. Technol.*, vol. 28, no. 2, Feb. 2017, Art. no. 025005.

[3] M. Kim, "Design of a new dual-mode torque standard machine using the principle of the Kibble balance," *IEEE Trans. Instrum. Meas.*, vol. 70, pp. 1–7, 2021.

[4] Z. Comden et al., "A new spin on Kibble: A self calibrating torque realization device at NIST," in *Proc. 22nd Int. Conf. Exhib.*, Geneva, Switzerland, 2022, pp. 349–352.

[5] L. Chao, F. Seifert, D. Haddad, J. Pratt, D. Newell, and S. Schlamminger, "The performance of the KIBB-g1 tabletop Kibble balance at NIST," *Metrologia*, vol. 57, no. 3, p. 10, 2020.

[6] S. Vasilyan et al., "The progress in development of the Planck-balance 2 (PB2): A tabletop Kibble balance for the mass calibration of E2 class weights," *tm-Technisches Messen*, vol. 88, no. 12, pp. 731–756, Dec. 2021.

[7] Z. Comden et al., "Continued development of an Si-traceable torque realization device," in *Proc. Conf. Precis. Electromagn. Meas.*, Wellington, New Zealand, 2022.

[8] D. Haddad et al., "Invited article: A precise instrument to determine the Planck constant, and the future kilogram," *Rev. Sci. Instrum.*, vol. 87, no. 6, Jun. 2016, Art. no. 061301.

[9] I. A. Robinson, "Towards the redefinition of the kilogram: A measurement of the Planck constant using the NPL mark II Watt balance," *Metrologia*, vol. 49, no. 1, pp. 113–156, Dec. 2011.

[10] J. Tellinghuisen, "Least squares methods for treating problems with uncertainty in x and y," *Anal. Chem.*, vol. 92, no. 16, pp. 10863–10871, Aug. 2020.

Zane Comden received the B.S. degree in physics from California Polytechnic University, Humboldt, Arcata, CA, USA, in 2018.

He spent a year in private industry before moving to the National Institute of Standards and Technology, Gaithersburg, MD, USA. He is currently a Physicist with the National Institute of Standards and Technology. His primary research interests include torque realization and development of the prototype electronic NIST torque realizer.

John Draganov received the B.S. degree in mechanical engineering and the Master of Engineering degree in robotics with an emphasis on control and automation from the University of Maryland, College Park, MD, USA, in 2020 and 2023, respectively.

From 2019 to 2022, he worked as a Contractor for an optical communication terminal focused startup. In 2022, he rejoined the NIST as a Mechanical Engineer in the FEM group, after a previous internship at the FEM group during his undergraduate program.

Stephan Schlamminger (Senior Member, IEEE) received the Diploma degree in physics from the University of Regensburg, Regensburg, Germany, in 1998, and the Ph.D. degree in experimental physics from the University of Zurich, Zürich, Switzerland, in 2002. His thesis was on the determination of the Newtonian constant of gravitation, G.

From 2002 to 2010, he worked with the University of Washington, Seattle, WA, USA, on an experimental test of the equivalence principle. In 2010, he moved to the National Institute of Standards and Technology (NIST), Gaithersburg, MD, USA, and began working on the Kibble balance. In 2016, he became the Leader of the Fundamental Electrical Measurement (FEM) Group. From 2017 to 2018, he was at the Regensburg University of Applied Science, Regensburg, where he taught physics. In 2018, he rejoined the NIST, where he is currently a Physicist with the FEM Group.

Frank Seifert was born in Berlin, Germany. He received the Dipl.-Ing. and Dr.-Ing. degrees in electrical engineering from the Leibniz University of Hannover, Hannover, Germany, in 2002 and 2009, respectively.

He was with the California Institute of Technology, Pasadena, CA, USA, from 2009 to 2012, where he was involved in research on the frequency stabilization of lasers for high precision metrology. He is currently with the National Institute of Standards and Technology, Gaithersburg, MD, USA, where he is involved in research on the Kibble balance.

Charles Waduwarage Perera received the bachelor's degree in electrical engineering from the University of Maryland, College Park, MD, USA, in 2018, and the Master of Science degree in electrical and computer engineering from Johns Hopkins University, Baltimore, MD, USA, in 2021.

While studying at the University of Maryland, he worked as a Research Assistant at the MEMS Sensors and Actuators Laboratory (MSAL), College Park. He joined the Applied Electrical Metrology Group, National Institute of Standards and Technology (NIST), Gaithersburg, MD, USA, in 2018, where he was responsible for designing, building, and testing circuitries for precision instrumentation systems to improve measurements in ac/dc difference, resistance, and voltage. His project involved research on Ingestible Capsule for Minimally Invasive Pancreatic Health Monitoring (Voyager), where he started to develop the interface between the sensors and microcontroller using Bluetooth.

David B. Newell received the Ph.D. degree in physics from the University of Colorado, Boulder, CO, USA, in 1994.

He worked on the Kibble balance project at the National Institute of Standards and Technology (NIST), Gaithersburg, MD, USA, as a National Research Council Post-Doctoral Fellow. He became a NIST staff member in 1996 and was the leader of the Fundamental Electrical Measurements Group, from 2004 to 2010 andagain since 2018. He has worked on measurements for the realization of micro- and nano-scale forces traceable to the SI, helped establish the use of graphene in quantum electrical standards, and worked on the construction of a new Kibble balance to realize the kilogram from a fixed value of the Planck constant. He chairs the CODATA Task Group on Fundamental Constants, which provided the exact values of the fundamental constants that form the foundation of the revised SI.

Dr. Newell is a member of the Philosophical Society of Washington and a fellow of the American Physical Society.

Leon S. Chao is currently a Mechanical Engineer with the National Institute of Standards and Technology, Gaithersburg, MD, USA. He served as the design engineer for the NIST-4 Kibble balance project which contributed to the redefinition of the kilogram in terms of a fixed value of the Planck constant. Recently, he leads two projects, the tabletop Kibble balance and electronic torque realizer, aimed at the development of commercial instrumentation for direct realization of mass and torque.